Journal of Evolutionary Biology, 2024, **37**, 1009–1022
https://doi.org/10.1093/jeb/voae085
Advance access publication 11 July 2024
Research Article

JOURNAL OF
Evolutionary Biology

eseb

Microbial artists: the role of parasite microbiomes in explaining colour polymorphism among amphipods and potential link to host manipulation

Célia Koellsch, Robert Poulin, Priscila M Salloum

Department of Zoology, University of Otago, Dunedin, New Zealand

Handling editor: Xiang-Yi Li Richter, Associate editor: Masahito Tsuboi

Corresponding author: Priscila Salloum, Department of Zoology, University of Otago, 340 Great King Street, Dunedin 9016, New Zealand. Email: priscila.madisalloum@otago.ac.nz

Abstract

Parasite infections are increasingly reported to change the microbiome of the parasitized hosts, while parasites bring their own microbes to what can be a multi-dimensional interaction. For instance, a recent hypothesis suggests that the microbial communities harboured by parasites may play a role in the well-documented ability of many parasites to manipulate host phenotype, and explain why the degree to which host phenotype is altered varies among conspecific parasites. Here, we explored whether the microbiomes of both hosts and parasites are associated with variation in host manipulation by parasites. Using colour quantification methods applied to digital images, we investigated colour variation among uninfected *Transorchestia serrulata* amphipods, as well as amphipods infected with *Plagiorhynchus allisonae* acanthocephalans and with a dilepidid cestode. We then characterized the bacteriota of amphipod hosts and of their parasites, looking for correlations between host phenotype and the bacterial taxa associated with hosts and parasites. We found large variation in amphipod colours, and weak support for a direct impact of parasites on the colour of their hosts. Conversely, and most interestingly, the parasite's bacteriota was more strongly correlated with colour variation among their amphipod hosts, with potential impact of amphipod-associated bacteria as well. Some bacterial taxa found associated with amphipods and parasites may have the ability to synthesize pigments, and we propose they may interact with colour determination in the amphipods. This study provides correlational support for an association between the parasite's microbiome and the evolution of host manipulation by parasites and host–parasite interactions more generally.

Keywords: parasite microbiome project, host–parasite interactions, parasite-induced host phenotype, microbiome, amphipod colour variation, acanthocephalan, cestode, bacteriota

Introduction

Although overlooked in most ecological and evolutionary studies, parasites have long been known to modulate behaviours and phenotypes in their parasitized hosts, with potential impacts at the host population level (Barber & Dingemanse, 2010; Herbison, 2017; Michalakis & Hochberg, 1994; Poulin, 2010). One example is hairworms (*Spinochordodes tellinii*) that induce water attraction in their grasshopper hosts (*Meconema thalassinum*), a remarkable adaptation for a worm that reproduces in water (Biron et al., 2005; Thomas et al., 2002). Mermithid nematodes also induce water attraction in various host species, in addition to feminizing their male mayfly hosts' secondary sexual characters (Herbison, Evans, Doherty & Poulin, 2019; Herbison, Evans, Doherty, Algie, et al., 2019; Vance, 1996). Some mechanisms underlying such behavioural/phenotypic manipulation have been attributed to parasite-induced differences in host gene expression and proteins that may interfere with the hosts' immune, nervous, or endocrine systems, with the expression of manipulation depending on individual and environmental circumstances (e.g., host and parasite sex, age, number of parasites, temperature, and pollution, presence of other parasite species; Poulin, 2010, Thomas et al., 2011). However, these factors fall short of explaining the wide variation of behaviour/phenotypic change induced by the same species of parasite in the same species of hosts, particularly within the same environment and population. In fact, large variation in the level of phenotypic manipulation was reported for parasites that benefit from their host's behavioural change (e.g., trophically transmitted parasites) and for parasites that induce nonadaptive behavioural changes in their hosts (e.g., as a consequence of pathology), highlighting that parasite-induced host behavioural manipulation does not result in fixed host phenotypes.

A hypothesis recently put forth considers the host's and parasite's microbiomes as potentially responsible for some of the parasitized host's behavioural/phenotypic modifications (Biron et al., 2015; Dheilly, Poulin, et al., 2015; Poulin et al., 2023). Branching from the holobiont context, in which an organism and its microbiome are seen as an integrated whole (Bordenstein & Theis, 2015; Roughgarden, 2020; Roughgarden et al., 2017; Theis et al., 2016), parasites, their hosts, and the microbiome of both would be the subject of co-evolution (Dheilly, 2014). Increasingly, microbiomes have been incorporated into studies of host–parasite interactions (Dheilly et al., 2017; Dheilly, Ewald, et al., 2019; Dheilly, Martinez, et al., 2019; Dheilly, Poulin, et al., 2015; Hahn & Dheilly, 2016), and found to modulate various aspects of the

Received February 4, 2024; revised May 16, 2024; accepted July 10, 2024

host-parasite dynamics, such as the parasite's infection success and the host's susceptibility to infection (Brealey et al., 2022; Dheilly et al., 2017; Dheilly, Poulin, et al., 2015; Hahn et al., 2022; Reverter et al., 2020; Reynolds et al., 2014, 2015; Salloum et al. 2023b; Tsagou et al., 2004). Microbiomes have also been associated with phenotypic modifications, for instance in the development of different castes of bees and trematodes, among many other examples (Balakirev et al., 2008; Carrier & Reitzel, 2018; Dheilly, Maure, et al., 2015; Hahn et al., 2022; Jorge, Dheilly, Froissard & Poulin, 2022; Lynch & Hsiao, 2019; Salloum et al. 2023a; Zoetendal et al., 2015). Furthermore, the microbiome of the same species of hosts differs when individuals are infected by different parasites species, indicating that infection (or the organism's response to infection) has an impact on the microbiome.

Here, we explored whether microbiome differences (focusing on bacteria) are associated with the phenotypic change presumably induced by parasites in their intermediate hosts. The rationale behind this idea is that, if the host microbiome changes in response to parasitic infection, then this change could also impact the phenotypic alterations they experience. Furthermore, parasites have their own microbiomes, which also interact with their surroundings, potentially impacting the parasite-induced host phenotypic change. In general, parasites have short generation times and, as such, are subject to fast evolution (Gandon & Michalakis, 2002). The microbial community associated with parasites must, therefore, benefit from the parasite's success (Van Vliet & Doebeli, 2019), even if this has a large cost for the microbiome (Roughgarden et al., 2017). Thus, changes in the parasitized host's behaviour/phenotype that benefit the parasite will also represent an advantage for the parasite-associated microbial taxa (Poulin et al., 2023, Salloum et al. 2023b), which could, for example, produce molecules that influence the parasitized host's phenotype/behaviour (Poulin et al., 2023). Given that microbiomes are largely variable even among conspecifics (Hahn et al., 2022; Jorge et al., 2020; Jorge, Dheilly, Froissard, Wainwright, et al., 2022; Jorge, Froissard, et al., 2022; Salloum et al., 2023), the final phenotype of the host would then result from the net effect of interactions among the parasite, the parasitized host, and their microbiomes (Dheilly et al. 2015; Poulin et al., 2023).

As a first step towards understanding the role of the microbiome in phenotypic changes induced by parasites in their hosts, we characterized the phenotype and bacterial community (hereafter bacteriota) of uninfected and infected hosts, as well as the bacteriota of the parasites infecting them. Our model system consists of *Transorchestia serrulata* amphipods (family Talitridae), which have high prevalence of infections by the acanthocephalan *Plagiorhynchus allisonae* and by a dilepidid cestode. These parasites have shore birds as their definitive hosts and are trophically transmitted when birds prey on infected amphipods (Figure 1, Lagrue et al., 2016). *Transorchestia serrulata* amphipods have various colour morphs, some of which have a higher prevalence of acanthocephalan (dark grey and blue) or cestode infections (dark grey and green, Lagrue et al., 2016). Given these different colours between infected and uninfected amphipods, it was hypothesized that the parasites induce colour changes in their amphipod hosts, making them more conspicuous to predators, increasing the chances that the parasite reaches its definitive host. Colours are conferred by pigments, which are part of metabolic processes that can be affected by subtle changes (Wigglesworth, 1949). These changes could result from the parasitic infection and alterations in the microbiome. We used quantified colours from digital images to test for an association between amphipod colour and infection status (uninfected, acanthocephalan-infected, and cestode-infected amphipods). More importantly, we explored whether the bacteriota of hosts and parasites are associated with the amphipod colours. As far as we know, this is the first test of the joint effects of host and parasite microbiomes on parasite-induced alterations in host phenotype.

Methods

Collection

Amphipods, sediment, and seawater were collected from the supralittoral zone at Lower Portobello Bay, Dunedin, New Zealand (45° 4,904,800 S, 170° 4,001,200 E) in March 2023. Approximately 500 individuals of all sizes from an area of ~8m² were manually gathered, placed in sterile 1 L plastic containers with sediment from the collection site (roughly 50 amphipods per container), and transported back to the laboratory in the Department of Zoology, University of Otago. Two environmental samples (substrate) were collected with sterile swabs, and stored on ice until arrival in the laboratory, where they were placed at −70 °C. Collected amphipods were housed alive in the collection containers, with 200 mg of sediment from the collection site which was kept moist with the collected sea water. Of all amphipods, 100 individuals were randomly sampled from the various containers and processed as below.

Photos and colour analyses

Given that colour morph classifications are subjective, particularly when there is large colour variation, we characterized *T. serrulata* phenotypes using quantified colour in digital images. To photograph the amphipods, animals were cold-stunned by placing the whole container (with the sediment) at—20°C for 20 min. Stunned amphipods (did not move once touched) were placed in-between microscope slides, which were held together by adhesive putty. The slides were submerged in sea water from the collection site in a sterile petri dish. Photos were taken under the dissecting microscope, using an AMSCOPE Microscope Digital Camera MU1003B (10MP aptina colour CMOS, ultra-fine colour engine) mounted on an Olympus SZ61 model SZ2-ILST dissecting microscope, with the same camera positioning, same (artificial) lighting conditions, and the same scale for all amphipods. A grey card, which is a standardized tone with two known colours (18 grey, 90 white) used in photography to obtain an accurate metre reading, was submerged and photographed under the same conditions.

The ImageJ v1.54d plug-in Mica Toolbox (Abràmoff et al., 2004; Troscianko & Stevens, 2015) was used to normalize all photos based on a sequential method (i.e., a grey card and the image are in separate photos), making colour comparable across different images. Settings for the image normalization can be found in the supplementary material. Normalized photos (saved as PNG files) were imported into Adobe Photoshop 2022 v25.5.2. In Photoshop, a standard black (RGB 0,0,0) background file was created with A4 size in landscape orientation, using RGB colour mode and selecting the option of "no colour profile management." Each normalized amphipod image was then loaded, the amphipod selected with the "quick

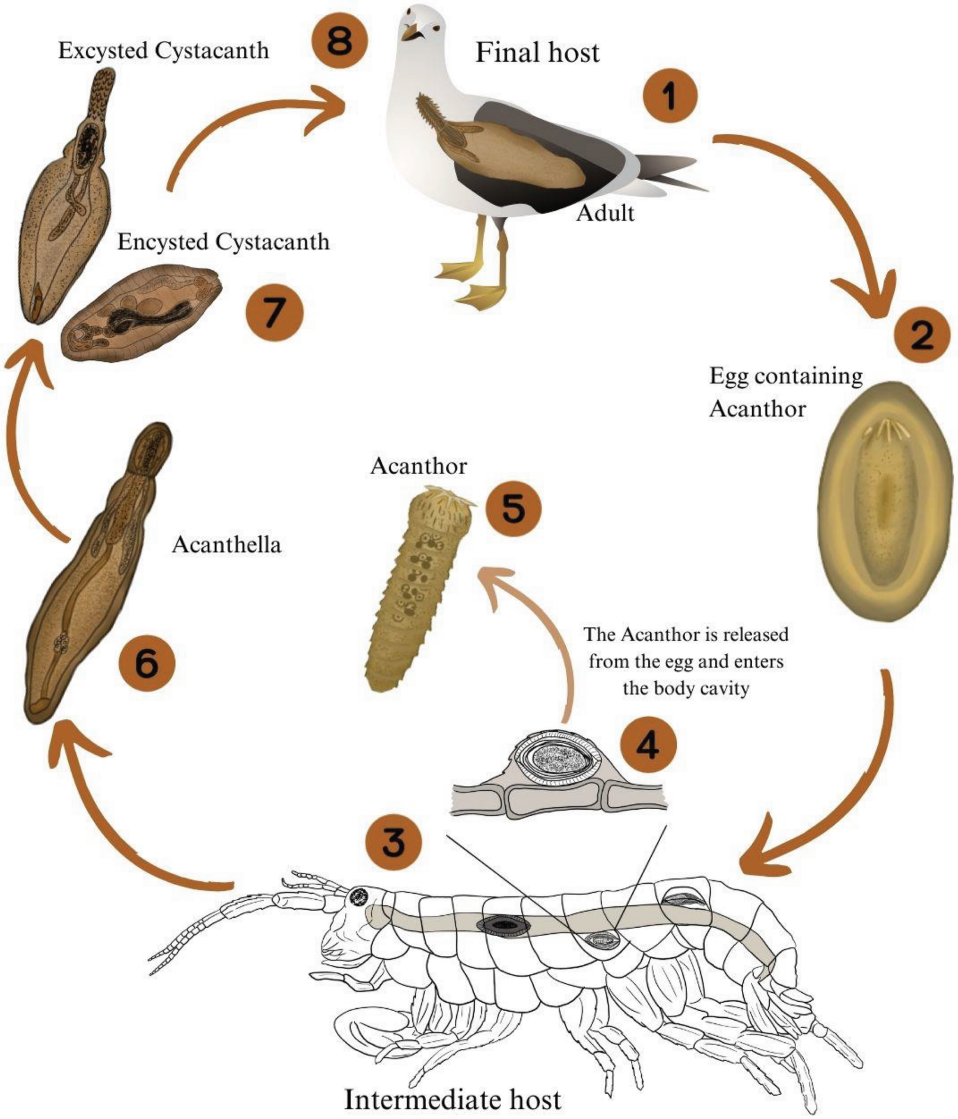

Figure 1. Life cycle of the acanthocephalan *Plagiorhynchus allisonae*. The same hosts are used by the dilepidid cestode. 1. *P. allisonae* eggs are released in the definitive hosts' faeces; 2. The eggs contain a fully developed Acanthor larva when excreted in faeces; 3. The eggs are ingested by an intermediate host, in this case *Transorchestia serrulata* amphipods; 4–5. The Acanthor is released from the egg and enters the haemocoel of the amphipod; 6. It then enters its second larval phase, called the Acanthella; 7. After 6–12 weeks, the acanthocephalan reaches the infective stage known as the Cystacanth; 8. The definitive host (gulls, oystercatchers, and rarely spoonbills) is infected when intermediate hosts containing infective Cystacanths are ingested. In the definitive host, the released juveniles attach themselves to the wall of the small intestine, where they mature and reproduce after about 8–12 weeks.

selection tool" (using a size of five pixels for the selection tool) and pasted on the black background file. In the black background, amphipods eyes and photography artefacts were removed (noise masking) by turning eyes, eggs, dirt, air bubbles, and potential photography artefacts into black background. Masked images were saved as PNG files and loaded into R v4.2.2 (R-Core-Team, 2022), with the packages PNG v. 0.1-8 (Urbanek, 2022) and colordistance v.1.1.2, for colour quantification and analyses.

Colour quantifications and analyses were undertaken based on two colour scales, the RGB (Red-Green-Blue) and the CIELab (a colour scale defined by the International Commission on Illumination, see below). The RGB scale is widely used in digital images, with a value of red, green, and blue in each pixel (Kendal et al., 2013). The RGB scale can be transformed into standardized, nonlinear, device-independent colour scales, of which an example is the International Commission on Illumination (CIE) L*a*b scale (hereafter CIELab, Kendal et al., 2013; McLaren, 2008). The "L" dimension represents luminance (dark to light), the "a" dimension represents the green to red spectrum, and the "b" dimension represents the blue to yellow spectrum (Kendal et al., 2013; McLaren, 2008). To convert the images to CIELab, the function convert_colour of the package grDevices v4.2.2 (R Core Team) was used, from sRGB to CIELab, specifying the illuminant as D65 (standard indirect day light). Summary statistics were then calculated for RGB and CIELab images, and analyses were undertaken with the mean and the maximum of each colour channel in each scale. Firstly, a principal component analysis was done with the prcomp base R function to check whether uninfected amphipods or amphipods infected by different parasites (acanthocephalan-infected and

cestode-infected) have different colours. Secondly, due to the non-normal distribution of residuals resulting from ANOVAs (Supplementary Tables S1 and S2), a Kruskal–Wallis test (Kruskal.test base R function) was done to check whether the different infection groups also differ in their RGB and CIELab colour values. Finally, a multinomial logistic regression was undertaken separately for each colour scale (RGB and CIELab) with the package Tidymodels v1.1.1 (Kuhn & Wickham, 2020), using each colour channel (R, G and B, or L, a and b) as independent variables and infection as the dependent variable. Model fit was evaluated based on deviance and AIC, and the false discovery rate was used to account for multiple testing.

To estimate colour distance among amphipods, the R package colordistance v.1.1.2 (Weller & Westneat, 2019) was used to bin the average colour value of each pixel into histograms, with each bin corresponding to a bar in the histogram and the number of bins assigned by the user. Once a distribution for each image was obtained (the histograms of each image), we estimated colour distance based on the Earth Mover's Distance method (EMD, Rubner et al., 2000). In brief, the EMD method compares colours among images by estimating the cost of transforming one colour distribution into another, so the larger the colour difference, the larger the cost (Rubner et al., 2000; Weller & Westneat, 2019). These analyses were performed in RGB scale. The black background was removed (with lower and upper RGB thresholds of 0 and 0.1, respectively). Two different settings were used: first a single bin per colour channel was used (1*1*1 = 1 bin in total); then, two bins per colour channel were used (2*2*2 = 8 bins in total). The number of bins per colour channel represents how many clusters are used to group pixels in a colour channel. For example, for the eight-binned dataset, each image was summarized by eight values of red, eight values of green, and eight values of blue. Colour distance between samples was estimated based on both the single-binned and the eight-binned dataset; heatmaps were plotted using the colordistance package, and neighbour joining trees were constructed with ape v 5.7-1 (Paradis & Schliep, 2019). The single-binned dataset was used in a multidimensional scaling analysis undertaken with vegan v 2.6-4, using the metaMDS function, Bray-Curtis distances, and 999 permutations. For the eight-binned dataset, multidimensional scaling analysis were undertaken based on the earth mover's (colour) distances and the following settings: maxit = 999, trymax = 500, wascores = TRUE, expand = TRUE.

Amphipod dissections, DNA extraction, PCR, and sequencing

Dissections were done under a UV-sterilized laminar flow hood. All material used was UV-sterilized, dissecting kits and solutions were autoclaved, and petri dishes were sterilized by soaking in 1:100 TriGene dilutions. Dissection instruments were sterilized by sequential immersion in 1:100 TriGene, 70% ethanol, and distilled water.

Amphipods were euthanized by freezing. To reduce contamination from the exterior of the amphipod's body, dead amphipods were stirred in 70% ethanol, dried with a paper tissue, and placed in a petri dish for dissection. A scalpel was used to remove the head, following which the dorsal part of the body (around the third scale) was opened, and haemolymph was collected with a sterile cotton swab and stored at—70 °C. Each amphipod was then carefully pulled apart and any endoparasites found were isolated. Parasites were counted, washed by pipetting up and down in phosphate-buffered saline (PBS) over a series of three wells of a culture plate (to reduce external contamination from the host's haemolymph on the parasite) and stored at—70°C. If more than one parasite was found, different taxa were stored separately (e.g., one tube for cestodes and another for acanthocephalans) and the same taxon was pooled (e.g., a single tube for more than one acanthocephalan from the same individual amphipod). A negative control for the PBS solution was taken (100 µL) and stored at –70 °C.

DNA extraction from hosts haemolymph and parasites, as well as for the PBS buffer negative control, was undertaken with the Qiagen Power Soil Kit following the manufacturer's recommendations, except that the bead-beating step was increased to 20 min and that parasites were incubated overnight at 60 °C with 20 µL of proteinase K (20 mg/mL) to lysate the cells. Two DNA negative controls were included. Library preparations were carried out as in Jorge et al. (2020), but amplicons were purified using Mag-Bind TotalPure NGS (Omega Bio-Tek) at a ratio of 0.8 bead solution to amplicon (PCR product). Two PCR negative controls were included. Amplicon concentrations were defined with a Qubit fluorometer, normalized to the lowest concentration, multiplexed, and sequenced, targeting the V4 hypervariable region of the bacterial 16S SSU rRNA gene with the primers 515F- 806R (Apprill et al., 2015; Parada et al., 2016) using an Illumina MiSeq platform and v3 reagent cartridge (250 bp, paired-end) at the Otago Genomics & Bioinformatics Facility.

Microbiome analyses

Bioinformatics

Quality of the demultiplexed sequences was checked using FastQC v0.11.9 and MultiQC v1.14. The cutadapt plugin implemented in QIIME2 v2023.5 (Bolyen et al., 2019) was used to remove primers and adaptors from raw sequences, with 0 error rate and minimum length of 190 bp. Sequences were forward- and reverse- trimmed by 13 bp, truncated at 170 bp (forward) and 190 bp (reverse), and denoized using the dada2 plugin in QIIME2 (Callahan et al., 2016). The SILVA database version 138.1 targeting the prokaryotic gene region SSURef_NR99 was trained on our dataset, using the Naïve Bayes classifier in QIIME2 and the same settings as Salloum et al. (2023). The data was then filtered to remove mitochondria, chloroplasts, eukaryotes, and sequence variants without a phylum assignment. Contamination was identified with the R package decontam v1.18.0 (Davis et al., 2018), using the 'either' method with a frequency threshold of 0.1 and a prevalence threshold of 0.5 (Supplementary Figures S10 and S11). This means that sequence variants were considered contaminants based on the distribution of the frequency of each variant as a function of the DNA input concentration (frequency method) and on whether prevalence of sequence variants is higher in negative controls (five negative controls in total) than in true samples (prevalence method with threshold 0.5). Sequence variants identified as contaminants were removed from the dataset. Rarefaction curves were done with a maximum of 4000 sequence variants per sample (depth) and various alpha diversity metrics (Faith's PD, Shannon Diversity, and number of observed sequence variants), using the *qiime diversity alpha-rarefaction* function in Qiime2. A depth cut-off was defined as a mid-point between sample size and the asymptote of the rarefaction curve (where the

increase in diversity levelled off in relation to the number of sequence variants, and not many amphipod samples were lost, Supplementary Figure S9), which resulted in a minimum total frequency of 500 sequence variants in a single sample with a minimum occurrence of two samples (found at least twice in the dataset). The filtered dataset has 71 amphipods (21 infected by acanthocephalans and 11 by cestodes) and 32 parasites (23 acanthocephalans and 9 cestodes).

The observed and expected composition of the ZymoBIOMICS microbial community standards were compared in QIIME2 with the plugin "quality control" to evaluate data quality (before filtering, Supplementary Figure S12). Taxonomy was assigned based on the trained SILVA database using the feature-classifier plugin with sklearn mode in QIIME2; amplicon sequence variants (ASVs) were aligned with MAFFT using the phylogeny plugin in QIIME2 and rooted and unrooted phylogenetic trees were built with FastTree2.

Statistical analyses

QIIME2 filtered output files were loaded into R v4.1.3 (R-Core-Team, 2022) using the packages qiime2R v0.99.6 and file2meco v0.6.0. Phyloseq v1.42.0 was used to group amplicon sequence variants (ASVs) into all higher taxonomic ranks (phylum, class, order, family, and genus). All analyses were undertaken with the package microeco v1.1.0 unless otherwise stated. Tests were corrected for multiple testing with the FDR method for a 0.05 significance level (standard in the microeco and other R packages used). The two environmental samples were excluded.

Beta diversity of amphipods' microbiome was estimated at all taxonomic ranks available (phylum, class, order, family, genera, and ASV), using presence–absence metrics (Jaccard and Unweighted Unifrac) and metrics that take taxa abundance into account (Bray Curtis and Weighted Unifrac). Significance was estimated using perMANOVAs. Comparisons were made among amphipods subdivided by colour groups, which were defined based on four clades in the colour neighbour joining tree with larger than 0.25 Earth Mover's Distance (EMD) on the eight-binned dataset. Parasite microbiomes were also subdivided by their hosts' colour groups. In addition, to test for differences in the bacteriota composition of amphipods and parasites, a beta diversity comparison was made among all amphipods, acanthocephalans, and cestodes. Shapiro tests implemented in Stats v. 4_4.2.2 (R-Core-Team, 2022) were used to test for normality of the distance matrices, including the EMD colour matrix for the RGB colour scale with eight bins, using untransformed and log-transformed data. These matrices were used in Mantel tests implemented in the R package vegan v. 2.6-4 (Oksanen et al., 2022) to test for association of microbiome distance with the EMD colour distance (of masked, eight-binned images), using the Spearman method and 9999 permutations to test significance. In addition, to check how much variance in colour EMD distances is accounted for by the microbiome distance, effect sizes were calculated for pairs of measurements (colour-microbiome distances) using the function eta_squared applied to ANOVAs in the package effectsize v.0.8.6. Finally, redundancy analyses (RDA) were undertaken to check how much of variance in the microbiome community data matrix (response variable) could be explained by the colour matrix (explanatory variable). Analyses were done separately for the single-binned RGB colour scale and mean CIELab colour scale, using the microeco function cal_ordination. Redundancy analyses were done for hosts and parasites at all taxonomic ranks, and significance of the RDA full model was assessed with ANOVA-like permutation tests (999 permutations, returning pseudo-*F* values). Multiple regressions of colour variables with ordination axes were done to check for correlation among them (colour as dependent variable and the ordination axes as explanatory variables), using the cal_ordination_envfit function in the microeco package. For these ANOVAs and multiple regressions, the false discovery rate was used to account for multiple testing.

Alpha diversity of amphipods' microbiomes was estimated at all taxonomic ranks using the following metrics: observed richness, ACE (O' Hara, 2005), Chao1 (Chiu et al., 2014), Simpson (Hill, 1973), InvSimpson (Hill, 1973), Shannon (Hill, 1973), and Faith's PD (Faith, 1992). Alpha diversity significance was determined based on ANOVAs. Groups tested were the same colour groups used for the beta diversity analyses (at least 0.25 EMD colour distance among groups).

To check for differential abundance of microbial taxa associated with amphipods and parasites of different colour groups, three tests were used: Aldex2_kw (Fernandes et al., 2014), with 999 bootstraps; LinDA, with a filter to remove taxa with no statistical power (minimum relative abundance of 0.005 at ASV level, and of 0.001 at all other taxonomic ranks); and Corncob v. 0.3.2 (Martin et al. 2020), with the "Wald" hypothesis testing procedure. Unique and shared sequence variants among colour groups were represented in Upset plots. Bar plots of relative abundance comparing colour groups, as well as comparing the microbiota of all amphipods with that of acanthocephalans and cestodes were done based on group means.

Results

Amphipod host colours and parasitic infection

Ninety-three amphipods were included in the colour analyses, 27 infected by acanthocephalans and 15 by cestodes (7 amphipods infected by both parasites were excluded). Amphipod colour only showed a minor association with parasitic infection for the mean "a" colour channel (red-green axis) in the CIELab scale, based on the Kruskal–Wallis test result (chi-squared = 8.2919, df = 2, p-value = 0.01583, Supplementary Table S3). The multinomial logistic regressions did not detect association between infection status and any colour channel (Supplementary Table S4), and the models had high AIC and deviance. Amphipods were also well distributed in PCA space regardless of infection status and colour scale used, with great overlap (Supplementary Figures S1–S4 and Supplementary Table S5).

Clusters of different colours were found based on the Earth Mover's Distances (EMDs), but clusters had uninfected and infected amphipods with both parasites (Supplementary Figures S5 and S6). These patterns were also recovered on the neighbour joining trees based on colour distances of the single-binned dataset (with all 93 amphipods, Supplementary Figure S7) and of the eight-binned dataset (only including 71 amphipods with microbiome data, Figure 2, Supplementary Figure S6), with both trees showing infected and uninfected amphipods at various colour distances. The widespread presence of parasites was also clear in the multidimensional scaling analyses, although a cluster of uninfected and cestode-infected amphipods was closer to the blue and green channels

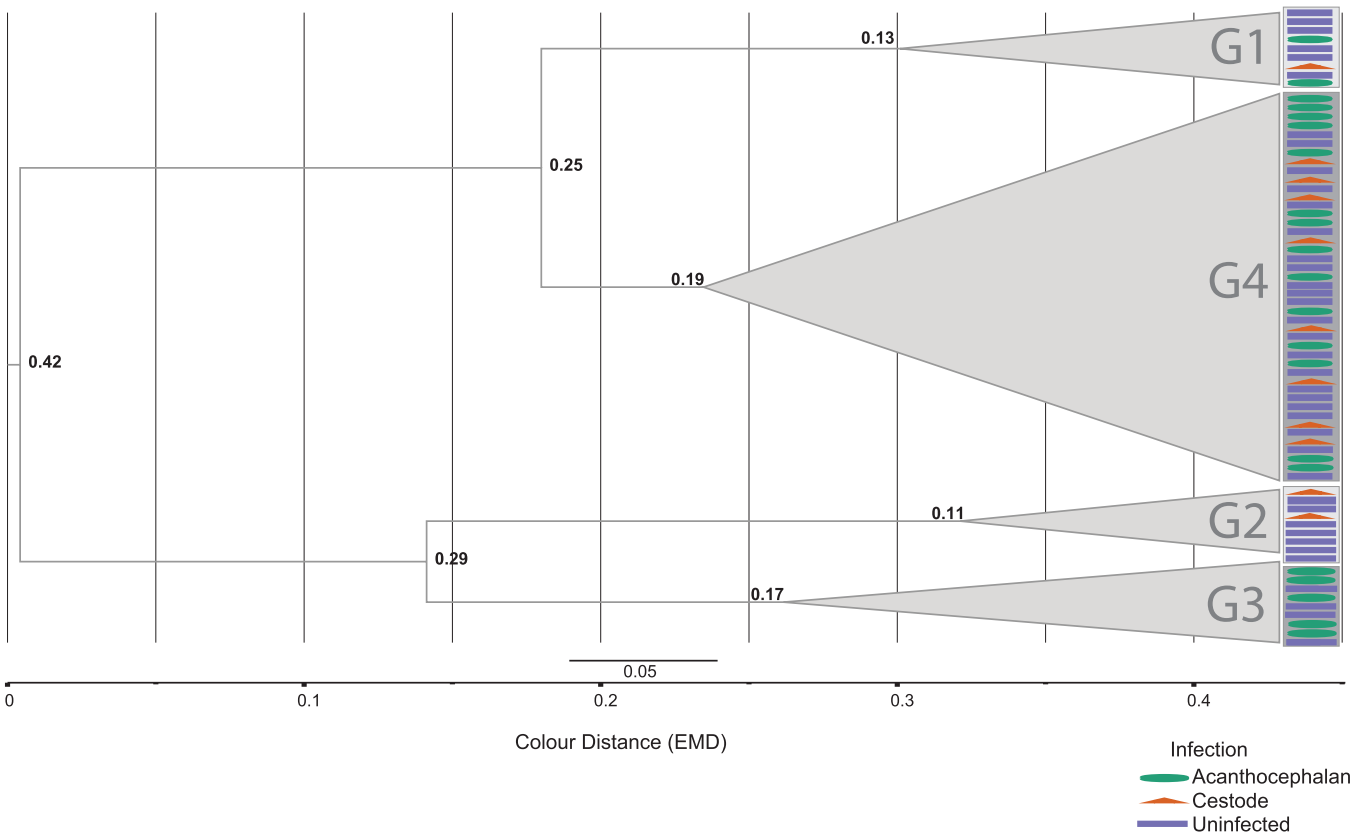

Figure 2. Neighbour joining tree based on Earth Mover's (EMD) colour distances (RGB scale, eight-bins dataset). G1 to G4 correspond to the colour groups into which amphipods were subdivided (colour distance greater than 0.25). Only amphipods that have microbiome data were included.

of the RGB scale in the first multidimensional scaling axis (Figure 3A and B). The multidimensional scaling stress for the one-binned and the eight-binned dataset was 0.051 and 0.16 respectively, with an overall better fit in the former (Supplementary Figure S8).

The four colour groups based on a colour distance larger than 0.25 EMD all contained uninfected amphipods (RGB scale, eight-bin dataset containing only 71 amphipods with microbiome data). One of the groups (G2) did not have acanthocephalan-infected amphipods, and another (G3) did not have cestode-infected amphipods (Figure 2).

Overall amphipod hosts and parasites microbiome results

The filtered dataset consisted of 71 amphipods and 32 parasites, ranging in depth from 553 to 950,911 (Table 1). Subdividing the parasite microbiome data by host colour group (with distances larger than 0.25 EMD) resulted in one group missing (G2), one group with most samples (G4, with 26 parasites), and two groups with small sample sizes (G1 with 2 samples and G3 with 5). Thus, parasites microbiomes were not assessed using host colour group as a categorical variable (e.g., for alpha and beta diversity) but were included when host colours were continuous variables (i.e., RGB colour scale, CIELab colour scale, and Earth Mover's Distance (EMD) colour distances). Mock community standard comparisons show high accuracy of taxonomic classification up to class level, decreasing for lower levels, although observed and expected abundances are highly correlated at all taxonomic levels (Supplementary Figure S12). The microbiome of amphipods, acanthocephalans and cestodes has different patterns of relative abundances (Supplementary Figure S13). In addition, beta diversity comparisons among amphipod hosts' bacteriota and that of acanthocephalans and cestodes showed differences in community composition, in particular between amphipods and acanthocephalan parasites, with more similarities between amphipods-cestodes and acanthocephalan-cestodes (Supplementary Table S6).

Amphipod host microbiomes and colours

Amphipod microbiomes subdivided by colour groups showed no differences in beta diversity (Supplementary Table S7, Figure 4A and B). All distance matrices at ASV level were not normally distributed (Supplementary Table S8). Mantel tests showed no association between colour distance and host microbiome distance (all p-values > 0.05, Supplementary Table S9). Effect sizes were all extremely small (to the order of 10e−3, Supplementary Table S10). All colour variables of amphipods (only including those with microbiome data available) were autocorrelated in the mean RGB scale (except for cestode-infected and acanthocephalan-infected mean red and blue, Supplementary Figure S14) and in the mean CIELab scale (except for acanthocephalan-infected mean L and mean a, Supplementary Figure S15). The proportion of the amphipod hosts' microbiome variance explained by colours in the RDA was from 1% to 5% (Supplementary Table S11) and the RDA full models were not significant for the colour matrices explaining variance in the constrained RDA variables (i.e., microbiome distances, Supplementary Table S12). However, multiple regression detected the

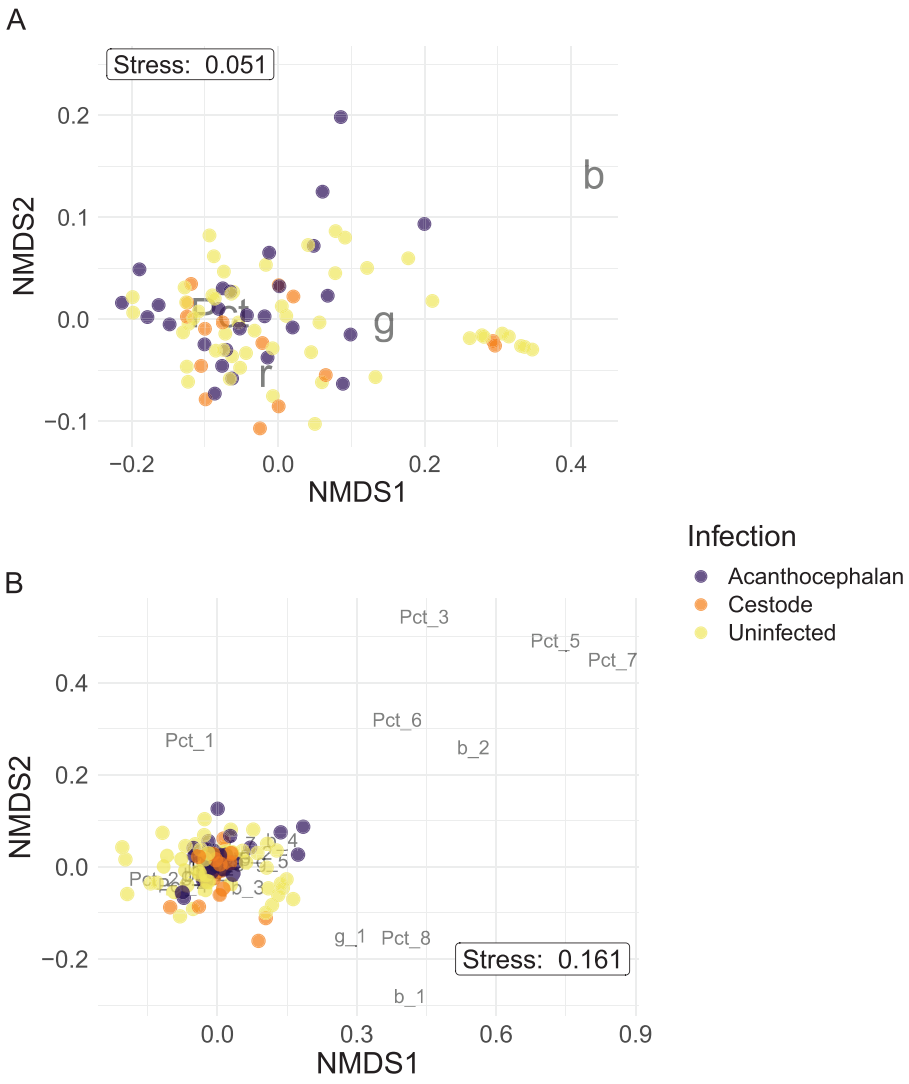

Figure 3. Multidimensional scaling analysis scores (points) and species (Pct, r, g, and b); r = red, g = green, b = blue, Pct = proportion of pixels explained by a bin. (A) Results of the one-binned dataset (Pct = 1 for all samples because this dataset contains a single bin); (B) Results of the eight-binned dataset.

Table 1. Filtered microbiome dataset overview.

Sample type	Sample size	Min number of ASVs	Max number of ASVs
Amphipods	71	553	923,631
Uninfected	39	662	923,631
Acanthocephalan-infected	21	553	90,852
Cestode-infected	11	1,017	28,182
Colour G1	9	588	165,151
Colour G2	8	900	56,287
Colour G3	10	1,814	90,852
Colour G4	44	553	923,631
Parasites	32	659	950,911
Acanthocephalans	23	659	45,065
Cestodes	9	3,919	950,911

Note. Group sample size and minimum (min) and maximum (max) number of ASVs in each group are presented.

mean red and mean L colour channels as potentially correlated with amphipod microbiome variance (p-values corrected for multiple testing (FDR) ranging from 0.009 to 0.1, Supplementary Table S13, Supplementary Figures S18 and S19). In the ordination space, of the 10 most abundant taxa, the most closely related with mean red were Spirosomaceae

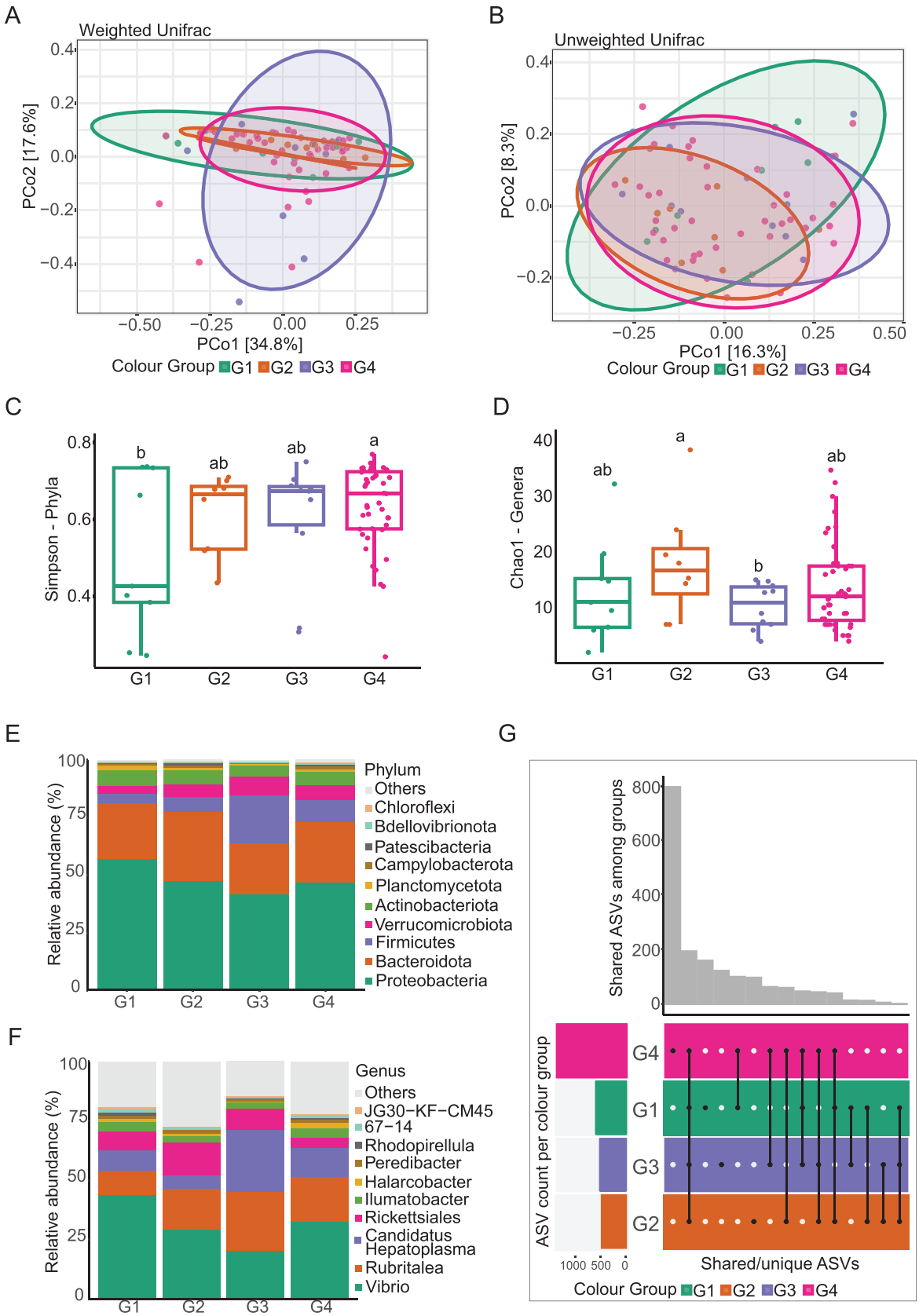

Figure 4. Comparisons of amphipod microbiomes among colour groups G1, G2, G3, and G4. (A) Beta diversity (Weighted Unifrac) at the amplicon sequence variant (ASV) level (nonsignificant result); (B) Beta diversity (Unweighted Unifrac) at the amplicon sequence variant (ASV) level (nonsignificant result); (C) Alpha diversity (Simpson) significant result, at phylum taxonomic rank; (D) Alpha diversity (Chao1) significant result, at genus taxonomic rank; (E) Mean phylum relative abundance per amphipod colour group, showing the 10 most abundant phyla; (F) Mean genus relative abundance per amphipod colour group, showing the 10 most abundant genera; (G) Upset plot comparing unique and shared amplicon sequence variants (ASVs) among the microbiomes of the amphipods subdivided by colour groups. The vertical bars represent the number of shared ASVs among the colour groups indicated with the filled (black) dots represented below them. The smaller horizontal bars on the left represent the number of ASVs found in each of the colour groups individually.

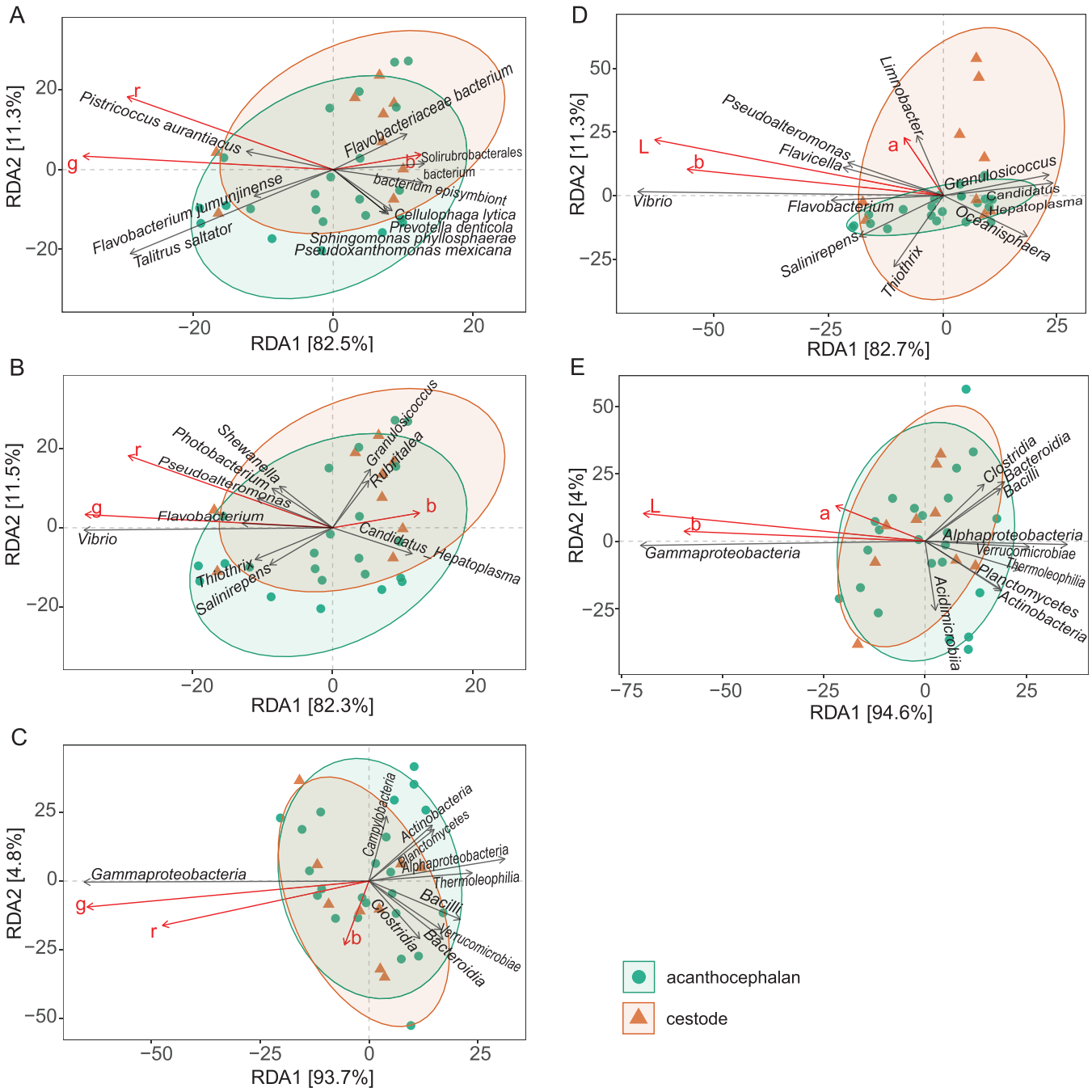

Figure 5. RDA on parasite microbiomes and mean amphipod host colours, using mean RGB and bacterial species (A), mean RGB and bacterial genus (B), mean RGB and bacterial class (C), mean CIELab and bacterial genus (D) and mean CIELab and bacterial class. Black arrows indicate the 10 most abundant taxa in the RDA space. Red arrows indicate the mean red (r), mean green (g), mean blue (b), mean L (L), mean a (a), and mean b (b) colours in the RDA space for each amphipod host (only including the 32 for which parasite bacteriome data is available). All plots represent significant results in the RDA1 axis. *Note*: In (A), *Talitrus saltator* is an incorrect species name in the Silva database v. 138.1, corresponding to sequences GDUJ01044859.40.1504, GDUJ01044860.143.1046, and GDUJ01044858.143.1623 of *Thiothrix* bacterial genus representatives, referred to as *Thiothrix* sp. in this study.

and Rickettsiales at family level (Supplementary Figure S18). Those in an opposite orientation from mean red in the RDA space were Rubritaleaceae at family level (Supplementary Figure S18). Amphipod-associated bacterial taxa correlated with the mean L colour variable in the RDA space were *Brumimicrobium glaciale*, *Clostridium perfringens* and *Flavobacteriaceae bacterium* at species level, *Photobacterium* at genus level, and Weeksellaceae and Spirosomaceae at family level (Supplementary Figure S19). Those in an opposite orientation from mean L in the RDA space included five taxa at species level (*Flavobacterium jumunjinense*, *Thiothrix* sp. (see caption on Figure 5), *Joostella marina*, *Bizionia halleyonensis*, and *Vibrio tapetis*), *Pseudoalteromonas* and *Candidatus_Hepatoplasma* at genus level, and Vibrionaceae and Pseudalteromonadaceae at family level (Supplementary Figure S19).

Alpha diversity was significantly different only at phylum (Simpson metric, indicating a difference between G1 and G4, Figure 4C, Supplementary Table S14) and genus taxonomic ranks (Chao1, indicating a difference between G2 and G3, Figure 4D, Supplementary Table S14). Differential abundance among amphipod colour groups was detected in some bacterial taxa with corncob and LinDA, but not with the Aldex2_kw approach (Supplementary Figures S20 and S21, Supplementary Tables S15 and S16). Corncob results indicated that the phylum Firmicutes was more abundant in G3 amphipods and Patescibacteria (or 'candidate phyla radiation') was less variable in this same colour group than in amphipods of other colour groups; the order Chitinophagales and the family NS9-marine-group (order Flavobacteriales, phylum Bacteroidota) were less variable in G2 amphipods than in amphipods of other colour groups; and the family Moraxellaceae (order Pseudomonadales, phylum Proteobacteria) was more abundant and more variable in G4 amphipods than in the others. In addition, there was differential abundance and variability in the class Gracilibacteria (phylum Patescibacteria) and the family Thiotrichaceae of order Thiotrichales (phylum Proteobacteria), but this was independent of the amphipod colour groups (that is, only the intercept was significant, Supplementary Table S15). The LinDA method detected significant differential abundance only at the ASV level (Supplementary Figure S21, Supplementary Table S16). ASVs corresponding to the family Sphingomonadaceae (phylum Proteobacteria) and to the genus *Taeseokella* (family Spirosomaceae, phylum Bacteroidota) were less abundant in G1 than G3 and G4 amphipods. Finally, an ASV corresponding to the family Weeksellaceae (phylum Bacteroidota) was less abundant in G1 than in G4 amphipods; Weeksellaceae were also positively correlated with amphipod mean L in the RDA.

The most abundant bacterial phyla were Proteobacteria and Bacteroidota. At genus rank, *Vibrio* (which has a species in an opposite orientation from mean L in the RDA) was followed closely by *Rubritalea* (Figure 4E and F). Colour group G4 had the largest number of samples (44 amphipods) and unique ASVs, followed by ASVs shared among all amphipods, and between any colour group with G4 (Figure 4G). The number of unique ASVs within each of the smaller colour groups (G1, G2, and G3) was larger than the number shared among them (excluding G4).

Parasite microbiomes and amphipod host colours

Mantel tests showed no association between host colour distance and parasite microbiome distance (all p-values > 0.05). Effect sizes were all extremely small (to the order of 10e−3). Some colour variables were autocorrelated for the 32 hosts having parasites with microbiome data (mean red and mean green in the mean RGB scale, and all colour variables in the mean CIELab scale, Supplementary Figures S16 and S17). However, an interesting result is that parasite microbiome distances were significantly explained by the constrained RDA axis 1 (Supplementary Tables S11 and S12). This axis explained a cumulative proportion of variance of 82.5% at species level, 82.3% at genus level, and 93.7% at class level (Figure 5), of which 8–10% were explained by the constraining mean RGB colour matrix (Supplementary Table S11). In addition, the RDA full model was significant at these three taxonomic ranks (species, genera, and class, Supplementary Table S11). The RDA of the mean RGB colour scale at species and genus level showed red and green colours in an opposite direction from blue, and two groups of bacterial taxa distributed more closely to either red-green or to blue. The species closer to the red-green axis were *Thiothrix* sp. (see caption in Figure 5), *Flavobacterium jumunjinense* and *Pistricoccus aurantiacus* (the first two also in a negative correlation with mean L in the host microbiome RDA); the genera closer to the red-green axis were *Salinirepens*, *Thiothrix*, *Vibrio*, *Flavobacterium* (also in a negative correlation with mean L in the host microbiome RDA), *Pseudoalteromonas* (also in a negative correlation with mean L in the host microbiome RDA), *Photobacterium* (also correlated with mean L in the parasite's microbiome RDA), and *Shewanella*; the species closer to the blue axis and in an opposite orientation from red and green in the RDA space were *Flavobacteriaceae bacterium* (also positively correlated with mean L in the host microbiome RDA), *Solirubrobacterales bacterium*, an unnamed species of Chitinophagales that is an epibiont of crabs (Zwirglmaier et al., 2014) termed '*bacterium_episymbiont*' in the Silva v138.1 database, *Prevotella denticola*, *Cellulophaga lytica*, *Pseudoxanthomonas Mexicana,* and *Sphingomonas phyllosphaerae*; and the genera closer to the blue axis were *Granulosicoccus*, *Rubritalea*, and *Candidatus_Hepatoplasma*. At class level, red, green, and blue point towards a similar direction, closer to Gammaproteobacteria. In addition, multiple regressions detected the host mean green colour (RGB scale) significantly correlated with the microbiome variance at ASV level in the RDA space (Supplementary Table S13). Variance in parasite microbiome distances were not correlated with the constrained RDA axis 1 of the host mean CIELab colour scale (Supplementary Table S12).

Discussion

The role of the microbiome in host–parasite interactions is increasingly considered in ecological parasitology studies, but the potential for microbiomes to interfere with parasite-induced host behavioural and phenotypic changes is largely underexplored. Based on previous evidence that acanthocephalan and cestode parasites change the colours of their *Transorchestia serrulata* amphipod hosts, we characterized the colour phenotype and bacteriota of uninfected, acanthocephalan-infected, and cestode-infected amphipods, as well as the bacteriota of their parasites. We found only a minor indication of an association between amphipod infection status and colour on the red-green axis (channel "a" of the CIELab scale), which could have been due to the amphipod's large colour variation and fewer than 100 amphipod individuals analysed. Host and parasite microbiome distances were not correlated with host colour distances. However, different host colour groups had specific bacterial taxa with differential abundance in each group, some of which were correlated with specific colour axes in the host bacteriota-host colour RDA (Weeksellaceae and the mean L colour channel). Finally, we found that the parasites' bacteriota correlated more strongly with host colour variation (in the RDA 1 axis of the parasite bacteriota-host colour RDA) than the amphipods' bacteriota (for which the RDA full model was not significant). It is worth noting that our methods assume that variation on the RGB and CIELab colour scales translates into some variation in what the amphipods predators (birds) perceive, and that the evidence we present, although suggestive of a link between

the microbiome of the parasite and amphipod host colour, is entirely correlational.

Acanthocephalans are known to modify the carotenoid content of other species of amphipods, resulting in colour differences (Drozdova et al., 2020; Hindsbo, 1972; Labaude et al., 2015). The mechanisms underlying such changes have been reported to involve carotenoid-binding proteins (Drozdova et al., 2020), but the total carotenoid content may also play a role. Some acanthocephalans can absorb carotenoid from their amphipod hosts (Barrett & Butterworth, 1968). In the case of cestodes, different crustacean species have certain colour morphs associated with higher infection rates (Lagrue et al., 2016; Sánchez et al., 2006). Bacteria are known to produce carotenoid pigments (e.g., *Pseudoalteromonas* species (Kusmita et al., 2017), a genus occurring in the amphipods' and the parasites' bacteriota). Thus, changes in the infected amphipod microbiome could be underlying differences in the carotenoid content, which would be perceived as variations in colour. Carotenoids have various roles in animals, including enhancing immunity (Maoka, 2020). Recently, pigments and immune regulation genes were found differentially expressed between trematode-infected and uninfected amphipods (Rand et al., 2023). Our results are only suggestive of potentially carotenoid-synthesizing bacteria in the amphipods' and parasites' microbiome. However, given that animals cannot synthesize carotenoids (Maoka, 2011), and carotenoids have an impact on animal immune systems (Maoka, 2020), it is possible that carotenoid-synthesizing bacteria interact with the amphipod's response to parasite infection. Furthermore, we found Rickettsialles in the amphipod bacteriota as potentially correlated with the red colour axis in the RDA. *Rickettsia* bacteria are known symbionts of aphids, and responsible for changing aphid colour from red to green (Tsuchida et al., 2010), via interference with the aphids' metabolism (Nikoh et al., 2018). Members of this bacterial family are also known pathogens of birds (Park & Poulin, 2020), which indicates they are probably able to colonize the definitive hosts of the parasites here studied (shore birds). Thus, these bacteria would not necessarily meet a dead end if their amphipod host were predated by a bird, and could even benefit from the amphipod's role as a vector of microorganisms to birds. Because of this, we cannot exclude a potential role of amphipod-associated bacteria in determining their colours, although our overall results provide weak support for a correlation between the amphipods' colour and their own microbiome.

Given that the only significant RDA result was from comparisons among parasites' microbiome distances with the amphipod host RGB colours, bacteria associated with the parasites could be involved in host colour determination. In this analysis, although the coefficient of correlation between the amphipod colour and the RDA1 axis was only between 0.08 and 0.1, this axis explained a large proportion of variation in the parasites' bacteriota. Furthermore, some bacteria associated with the parasites are closely related to pigment-producing taxa. For example, melanin production was identified in *Shewanella colwelliana* and in *Vibrio cholerae* (Nosanchuk et al., 2003). These two species belong to genera matching components of the parasites' bacteriota correlated with the amphipod red-green colour axis. If the bacterial sequences here identified belong to melanin producing taxa, and such melanin was found extracellularly, it could explain (at least partly) amphipod colour differences. Among its various functions, melanin has been correlated with bacterial pathogenicity and reported to help bacteria to avoid host immune response (Nosanchuk et al., 2003). In insects, melanin in haemolymph has antimicrobial activity (Nosanchuk et al., 2003), something that could be true for the amphipods as well. In the parasites, we also detected bacterial groups that were previously reported to produce carotenoids, such as *Pseudoalteromonas* (Kusmita et al., 2017) and *Rubritalea* (Yoon et al., 2007). *Pseudalteromonas* from the parasites were associated with the direction of the "a' (red-green) axis (also the L axis from hosts bacteriota), which represent colours conferred by carotenoids (yellow, orange, red and purple colours, Maoka, 2020). Taxa assigned to *Pseudoaltermonoas* were also found in negative correlation with the red-green axis, and more closely oriented towards the blue axis (*Pseudoalteromonas mexicana* in the parasites" bacteriota). Among other reasons, this apparent contradiction highlights the uncertainty of taxonomic classifications based on a small fragment of the 16S gene when finer taxonomic resolution would be more informative, as well as the fact that not all species and strains in a prokaryotic genus will have the same traits (Martiny et al., 2015; Oliver et al., 2023). However, given the known pigment production ability of closely related bacterial taxa to those here detected in association with parasites, further investigations of the potential of these taxa to interact with the parasites and modify amphipod host colours is warranted.

Rickettsia, *Rubritalea,* and *Vibrio* bacterial genera associated with parasites, in addition to *Candidatus_Hepatoplasma* (a known symbiont of amphipods, isopods and crabs, Chan et al., 2021; Leclercq et al., 2014; Sun et al., 2020), were the most abundant genera in all amphipods (Figure 4F), but the relative abundance of these genera differed among the amphipod colour groups. Even though the colour groups were arbitrarily categorized and may not be biologically meaningful, they represent larger colour distances than those between amphipods within each of those groups. Beta diversity showed no differences in host microbiome composition among these arbitrary colour groups, and the two significant alpha diversity results are also confounded with other variables (G1 and G4 are confounded by the larger number of amphipods in G4; G2 and G3 are missing acanthocephalan- and cestode-infected amphipods respectively). Similarly, the differential abundance tests were also based on the arbitrary colour groups, and results could have been confounded by these other factors. However, an interesting class recovered in differential abundance is the uncultured Gracilibacteria, which only contains bacteria of reduced metabolic capacities that have been suggested to be both symbionts and parasites. Gracillibacteria could be an obligate symbiont/parasite of amphipods, and differences in its abundance could have biological implications for the amphipods, and may or may not interfere with parasitic infections.

If the impact of parasite-induced behavioural and phenotypic change on the ecology and evolution of populations has been overlooked, that of the microbiome in such interactions has been almost completely ignored. This study has found correlative evidence for an association between colour variation among amphipod hosts and the bacteriota of both amphipods and their parasites, with weaker indication for an impact of the amphipods own bacteriota than that of their parasites on amphipod colour determination. Some bacteria here associated with colour differences were closely related or belong to taxa known to izesynthesize pigments. These

correlations align with the hypothesis that the bacterial communities of hosts and parasites may influence the phenotypic manipulation of parasitized hosts, something that has long been considered a unique adaptation of parasites (see Poulin et al., 2023). There is increasing evidence that microbiomes modulate their hosts phenotypes and are a factor driving phenotypic plasticity, which in turn may impact hosts communities and ecosystems as the object of evolution (Decaestecker et al., 2024). Our study expands on this context by showing potential for microbiomes to drive plasticity in phenotypes of organisms other than those of their associated hosts (i.e., parasites' microbiomes interacting with the parasitized hosts' phenotypes). Furthermore, if these changes in colour translate into a change in predation rate by birds, as shown in other systems (Hernández-Agüero et al., 2020; Nokelainen et al., 2014), there is potential for an impact of parasites microbiome at the macro-organismal community level. We believe amphipods of various species are great models to help further understand such complex interactions, given a wealth of parasitological knowledge on phenotypic and behavioural changes in parasitized amphipods, as well as the diversity of parasites that use them as intermediate hosts. Further studies characterizing the microbiomes of parasitized amphipods and of their parasites, as well as experimental infections and manipulations (e.g., with different antibiotics) will help shed light on the specific microbial players involved in such multi-dimensional interactions. Furthermore, colours are important traits in various systems, underlying many predator-prey interactions (aposematism, mimicry, crypsis) and driving evolution via sexual selection. Future research must consider the influence of the microbiome in shaping colour differences, which could, in fact, have an impact on our understanding of colour evolution.

Supplementary material

Supplementary material is available at *Journal of Evolutionary Biology* online.

Data availability

Raw sequence reads are available in the SRA (BioProject PRJNA1070336); raw and masked images, bioinformatics scripts, filtered data, FastQC reports, and metadata are available on Figshare (DOI: 10.6084/m9.figshare.25106309).

Author contributions

Célia Koellsch-Amet (Data curation [Lead], Formal analysis [Equal], Investigation [Equal], Methodology [Equal], Project administration [Equal], Software [Equal], Visualization [Equal], Writing—original draft [Equal]), Robert Poulin (Conceptualization [Lead], Funding acquisition [Lead], Project administration [Equal], Resources [Equal], Supervision [Equal], Writing—original draft [Supporting]), and Priscila Salloum (Conceptualization [Equal], Data curation [Supporting], Formal analysis [Equal], Investigation [Equal], Methodology [Equal], Project administration [Supporting], Resources [Supporting], Software [Equal], Supervision [Equal], Visualization [Equal], Writing—original draft [Equal])

Funding

This research was funded by a Marsden Fund grant (Royal Society of New Zealand, contract UOO2113), awarded to RP.

Acknowledgments

We acknowledge the use of the New Zealand eScience Infrastructure (NeSI) high performance computing facilities (https://www.nesi.org.nz). This work is part of a larger project, for which consultation was undertaken with local representatives of indigenous peoples (Ngāi Tahu).

Conflicts of interest

None declared.

References

Abràmoff, M. D., Magalhães, P. J., & Ram, S. J. (2004). Image processing with ImageJ. *Biophotonics International*, *11*(7), 36–42.

Apprill, A., McNally, S., Parsons, R., & Weber, L. (2015). Minor revision to V4 region SSU rRNA 806R gene primer greatly increases detection of SAR11 bacterioplankton. *Aquatic Microbial Ecology*, *75*(2), 129–137. https://doi.org/10.3354/ame01753

Balakirev, E. S., Pavlyuchkov, V. A., & Ayala, F. J. (2008). DNA variation and symbiotic associations in phenotypically diverse sea urchin *Strongylocentrotus intermedius*. *Proceedings of the National Academy of Sciences of the United States of America*, *105*(42), 16218–16223. https://doi.org/10.1073/pnas.0807860105

Barber, I., & Dingemanse, N. J. (2010). Parasitism and the evolutionary ecology of animal personality. *Philosophical Transactions of the Royal Society of London, Series B: Biological Sciences*, *365*(1560), 4077–4088. https://doi.org/10.1098/rstb.2010.0182

Barrett, J., & Butterworth, P. E. (1968). The carotenoids of *Polymorphus minutus* (Acanthocephala) and its intermediate host, *Gammarus Pulex*. *Comparative Biochemistry and Physiology*, *27*(2), 575–581. https://doi.org/10.1016/0010-406x(68)90254-5

Biron, D. G., Bonhomme, L., Coulon, M., & Øverli, O. (2015). Microbiomes, plausible players or not in alteration of host behavior. *Frontiers in Microbiology*, *5*, 775–780. https://doi.org/10.3389/fmicb.2014.00775

Biron, D. G., Marché, L., Ponton, F., … Thomas, F. (2005). Behavioural manipulation in a grasshopper harbouring hairworm: A proteomics approach. *Proceedings Biological Sciences*, *272*(1577), 2117–2126. https://doi.org/10.1098/rspb.2005.3213

Bolyen, E., Rideout, J. R., Dillon, M. R., … Caporaso, J. G. (2019). Reproducible, interactive, scalable and extensible microbiome data science using QIIME 2. *Nature Biotechnology*, *37*(8), 852–857. https://doi.org/10.1038/s41587-019-0209-9

Bordenstein, S. R., & Theis, K. R. (2015). Host biology in light of the microbiome: Ten principles of holobionts and hologenomes. *PLoS Biology*, *13*(8), e1002226. https://doi.org/10.1371/journal.pbio.1002226

Brealey, J. C., Lecaudey, L. A., Kodama, M., … August, A. (2022). Microbiome "inception": An intestinal cestode shapes a hierarchy of microbial communities nested within the host. *mBio*, *13*(3), e00679–e00622. https://doi.org/10.1128/mbio.00679-22

Callahan, B. J., McMurdie, P. J., Rosen, M. J., … Holmes, S. P. (2016). DADA2: High-resolution sample inference from Illumina amplicon data. *Nature Methods*, *13*(7), 581–583. https://doi.org/10.1038/nmeth.3869

Carrier, T. J., & Reitzel, A. M. (2018). Convergent shifts in host-associated microbial communities across environmentally elicited phenotypes. *Nature Communications*, *9*(1), 952–961. https://doi.org/10.1038/s41467-018-03383-w

Chan, J., Geng, D., Pan, B., … Xu, Q. (2021). Metagenomic insights into the structure and function of intestinal microbiota of the Hadal amphipods. *Frontiers in Microbiology*, *12*, 668989. https://doi.org/10.3389/fmicb.2021.668989

Chiu, C. -H., Wang, Y. -T., Walther, B. A., & Chao, A. (2014). An improved nonparametric lower bound of species richness via a modified good–turing frequency formula. *Biometrics*, *70*(3), 671–682. https://doi.org/10.1111/biom.12200

Davis, N. M., Proctor, D. M., Holmes, S. P., … Callahan, B. J. (2018). Simple statistical identification and removal of contaminant sequences in marker-gene and metagenomics data. *Microbiome*, *6*(1), 226. https://doi.org/10.1186/s40168-018-0605-2

Decaestecker, E., Van de Moortel, B., Mukherjee, S., … De Meester, L. (2024). Hierarchical eco-evo dynamics mediated by the gut microbiome. *Trends in Ecology & Evolution*, *39*(2), 165–174. https://doi.org/10.1016/j.tree.2023.09.013

Dheilly, N. M. (2014). Holobiont–holobiont interactions: Redefining host–parasite interactions. *PLoS Pathogens*, *10*(7), e1004093. https://doi.org/10.1371/journal.ppat.1004093

Dheilly, N. M., Bolnick, D., Bordenstein, S., … Rosario, K. (2017). Parasite microbiome project: Systematic investigation of microbiome dynamics within and across parasite-host interactions. *mSystems*, *2*(4), e00050–e00017. https://doi.org/10.1128/mSystems.00050-17

Dheilly, N. M., Ewald, P. W., Brindley, P. J., … Thomas, F. (2019). Parasite-microbe-host interactions and cancer risk. *PLoS Pathogens*, *15*(8), e1007912. https://doi.org/10.1371/journal.ppat.1007912

Dheilly, N. M., Martinez, M. J., Rosario, K., … Thompson, L. R. (2019). Parasite microbiome project: Grand challenges. *PLoS Pathogens*, *15*(10), e1008028. https://doi.org/10.1371/journal.ppat.1008028

Dheilly, N. M., Maure, F., Ravallec, M., … Mitta, G. (2015). Who is the puppet master? Replication of a parasitic wasp-associated virus correlates with host behaviour manipulation. *Proceedings Biological Sciences*, *282*(1803), 20142773. https://doi.org/10.1098/rspb.2014.2773

Dheilly, N. M., Poulin, R., & Thomas, F. (2015). Biological warfare: Microorganisms as drivers of host–parasite interactions. *Infection, Genetics and Evolution*, *34*, 251–259. https://doi.org/10.1016/j.meegid.2015.05.027

Drozdova, P., Saranchina, A., Morgunova, M., … Timofeyev, M. (2020). The level of putative carotenoid-binding proteins determines the body color in two species of endemic Lake Baikal amphipods. *PeerJ*, *8*, e9387. https://doi.org/10.7717/peerj.9387

Faith, P. D. (1992). Conservation evaluation and phylogenetic diversity. *Biological Conservation*, *61*(1), 1–10. https://doi.org/10.1016/0006-3207(92)91201-3

Fernandes, A. D., Reid, J. N. S., Macklaim, J. M., … Gloor, G. B. (2014). Unifying the analysis of high-throughput sequencing datasets: Characterizing RNA-seq, 16S rRNA gene sequencing and selective growth experiments by compositional data analysis. *Microbiome*, *2*(15), 1–13. https://doi.org/10.1186/2049-2618-2-15

Gandon, S., & Michalakis, Y. (2002). Local adaptation, evolutionary potential and host–parasite coevolution: Interactions between migration, mutation, population size and generation time. *Journal of Evolutionary Biology*, *15*(3), 451–462. https://doi.org/10.1046/j.1420-9101.2002.00402.x

Hahn, M. A., & Dheilly, N. M. (2016). Experimental models to study the role of microbes in host–parasite interactions. *Frontiers in Microbiology*, *7*, 1300. https://doi.org/10.3389/fmicb.2016.01300

Hahn, M. A., Piecyk, A., Jorge, F., … Dheilly, N. M. (2022). Host phenotype and microbiome vary with infection status, parasite genotype, and parasite microbiome composition. *Molecular Ecology*, *31*(5), 1577–1594. https://doi.org/10.1111/mec.16344

Herbison, R., Evans, S., Doherty, J. F., … Poulin, R. (2019). A molecular war: Convergent and ontogenetic evidence for adaptive host manipulation in related parasites infecting divergent hosts. *Proceedings Biological Sciences*, *286*(1915), 20191827. https://doi.org/10.1098/rspb.2019.1827

Herbison, R. E. H. (2017). Lessons in mind control: Trends in research on the molecular mechanisms behind parasite-host behavioral manipulation. *Frontiers in Ecology and Evolution*, *5*, 102. https://doi.org/10.3389/fevo.2017.00102

Herbison, R. E. H., Evans, S., Doherty, J. F., & Poulin, R. (2019). Let's go swimming: Mermithid-infected earwigs exhibit positive hydrotaxis. *Parasitology*, *146*(13), 1631–1635. https://doi.org/10.1017/S0031182019001045

Hernández-Agüero, J. A., Polo, V., García, M., … Cayuela, L. (2020). Effects of prey colour on bird predation: An experiment in Mediterranean woodlands. *Animal Behaviour*, *170*, 89–97. https://doi.org/10.1016/j.anbehav.2020.10.017

Hill, M. O. (1973). Diversity and evenness: A unifying notation and its consequences. *Ecology*, *54*(2), 427–432. https://doi.org/10.2307/1934352

Hindsbo, O. (1972). Effects of *Polymorphus* (Acanthocephala) on colour and behaviour of *Gammarus lacustris*. *Nature*, *238*(5363), 333–333. https://doi.org/10.1038/238333a0

Jorge, F., Dheilly, N. M., Froissard, C., & Poulin, R. (2022). Association between parasite microbiomes and caste development and colony structure in a social trematode. *Molecular Ecology*, *31*(21), 5608–5617. https://doi.org/10.1111/mec.16671

Jorge, F., Dheilly, N. M., Froissard, C., … Poulin, R. (2022). Consistency of bacterial communities in a parasitic worm: Variation throughout the life cycle and across geographic space. *Microbial Ecology*, *83*(3), 724–738. https://doi.org/10.1007/s00248-021-01774-z

Jorge, F., Dheilly, N. M., & Poulin, R. (2020). Persistence of a core microbiome through the ontogeny of a multi-host parasite. *Frontiers in Microbiology*, *11*, 954–967. https://doi.org/10.3389/fmicb.2020.00954

Jorge, F., Froissard, C., Dheilly, N. M., & Poulin, R. (2022). Bacterial community dynamics following antibiotic exposure in a trematode parasite. *International Journal for Parasitology*, *52*(5), 265–274. https://doi.org/10.1016/j.ijpara.2021.11.006

Kendal, D., Hauser, C. E., Garrard, G. E., … Moore, J. L. (2013). Quantifying plant colour and colour difference as perceived by humans using digital images. *PLoS One*, *8*(8), e72296. https://doi.org/10.1371/journal.pone.0072296

Kuhn, M., & Wickham, H. (2020). Tidymodels: A collection of packages for modeling and machine learning using tidyverse principles. R. package. https://www.tidymodels.org/.

Kusmita, L., Mutiara, E. V., Nuryadi, H., … Radjasa, O. K. (2017). Characterization of carotenoid pigments from bacterial symbionts of soft-coral *Sarcophyton* sp. from North Java Sea. *International Aquatic Research*, *9*(1), 61–69. https://doi.org/10.1007/s40071-017-0157-2

Labaude, S., Cezilly, F., Tercier, X., & Rigaud, T. (2015). Influence of host nutritional condition on post-infection traits in the association between the manipulative acanthocephalan *Pomphorhynchus laevis* and the amphipod *Gammarus pulex*. *Parasites & Vectors*, *8*, 403. https://doi.org/10.1186/s13071-015-1017-9

Lagrue, C., Heaphy, K., Presswell, B., & Poulin, R. (2016). Strong association between parasitism and phenotypic variation in a supralittoral amphipod. *Marine Ecology Progress Series*, *553*, 111–123. https://doi.org/10.3354/meps11752

Leclercq, S., Dittmer, J., Bouchon, D., & Cordaux, R. (2014). Phylogenomics of "*Candidatus Hepatoplasma crinochetorum*," a lineage of mollicutes associated with noninsect arthropods. *Genome Biology and Evolution*, *6*(2), 407–415. https://doi.org/10.1093/gbe/evu020

Lynch, J. B., & Hsiao, E. Y. (2019). Microbiomes as sources of emergent host phenotypes. *Science*, *365*(6460), 1405–1409. https://doi.org/10.1126/science.aay0240

Maoka, T. (2011). Carotenoids in marine animals. *Marine Drugs*, *9*(2), 278–293. https://doi.org/10.3390/md9020278

Maoka, T. (2020). Carotenoids as natural functional pigments. *Journal of Natural Medicines*, *74*(1), 1–16. https://doi.org/10.1007/s11418-019-01364-x

Martin, B. D., Witten, D., & Willis, A. D. (2020). *Modeling microbial abundances and dysbiosis with beta-binomial regression*. *Annals of Applied Sciences*, *14*(91), 4–115.

Martiny, J. B., Jones, S. E., Lennon, J. T., & Martiny, A. C. (2015). Microbiomes in light of traits: A phylogenetic perspective. *Science*, *350*(6261), aac9323. https://doi.org/10.1126/science.aac9323

McLaren, K. (2008). XIII—The development of the CIE 1976 (L* a* b*) uniform colour space and colour-difference formula. *Journal of the Society of Dyers and Colourists*, *92*(9), 338–341. https://doi.org/10.1111/j.1478-4408.1976.tb03301.x

Michalakis, Y., & Hochberg, M. E. (1994). Parasitic effects on host life-history traits: A review of recent studies. *Parasite*, *1*(4), 291–294. https://doi.org/10.1051/parasite/1994014291

Nikoh, N., Tsuchida, T., Maeda, T., … Fukatsu, T. (2018). Genomic insight into symbiosis-induced insect color change by a facultative

bacterial endosymbiont, "*Candidatus Rickettsiella viridis*.". *mBio*, *9*(3), e00890–e00818. https://doi.org/10.1128/mBio.00890-18
Nokelainen, O., Valkonen, J., Lindstedt, C., & Mappes, J. (2014). Changes in predator community structure shifts the efficacy of two warning signals in Arctiid moths. *The Journal of Animal Ecology*, *83*(3), 598–605. https://doi.org/10.1111/1365-2656.12169
Nosanchuk, J. D., & Casadevall, A. (2003). The contribution of melanin to microbial pathogenesis. *Cellular Microbiology*, *5*(4), 203–223. https://doi.org/10.1046/j.1462-5814.2003.00268.x
O' Hara, R. B. (2005). Species richness estimators: How many species can dance on the head of a pin? *Journal of Animal Ecology*, *74*, 375–386. https://doi.org/10.1111/j.1365-2656.2005.00940.x
Oksanen, J., Simpson, G., Blanchet, F. G., ... Weedon, J. (2022). Vegan community ecology package. R. package. https://CRAN.R-project.org/package=vegan
Oliver, A., Kay, M., & Lemay, D. G. (2023). TaxaHFE: A machine learning approach to collapse microbiome datasets using taxonomic structure. *Bioinformatics Advances*, *3*(1), vbad165. https://doi.org/10.1093/bioadv/vbad165
Parada, A. E., Needham, D. M., & Fuhrman, J. A. (2016). Every base matters: Assessing small subunit rRNA primers for marine microbiomes with mock communities, time series and global field samples. *Environmental Microbiology*, *18*(5), 1403–1414. https://doi.org/10.1111/1462-2920.13023
Paradis, E., & Schliep, K. (2019). ape 5.0: An environment for modern phylogenetics and evolutionary analyses in R. *Bioinformatics*, *35*(3), 526–528. https://doi.org/10.1093/bioinformatics/bty633
Park, E., & Poulin, R. (2020). Widespread Torix Rickettsia in New Zealand amphipods and the use of blocking primers to rescue host COI sequences. *Scientific Reports*, *10*(1), 16842. https://doi.org/10.1038/s41598-020-73986-1
Poulin, R. (2010). Parasite manipulation of host behavior. *Advances in the Study of Behavior*, *41*, 151–186.
Poulin, R., Jorge, F., & Salloum, P. M. (2023). Inter-individual variation in parasite manipulation of host phenotype: A role for parasite microbiomes? *The Journal of Animal Ecology*, *92*(4), 807–812. https://doi.org/10.1111/1365-2656.13764
Rand, D. M., Nunez, J. C. B., Williams, S., … Cardon, Z. G. (2023). Parasite manipulation of host phenotypes inferred from transcriptional analyses in a trematode-amphipod system. *Molecular Ecology*, *32*(18), 5028–5041. https://doi.org/10.1111/mec.17093
R-Core-Team. (2022). *R: A language and environment for statistical computing*. R Foundation for Statistical Computing.
Reverter, M., Sasal, P., Suzuki, M. T., … Tapissier-Bontemps, N. (2020). Insights into the natural defenses of a coral reef fish against gill ectoparasites: Integrated metabolome and microbiome approach. *Metabolites*, *10*(6), 227. https://doi.org/10.3390/metabo10060227
Reynolds, L. A., Finlay, B. B., & Maizels, R. M. (2015). Cohabitation in the intestine: Interactions among helminth parasites, bacterial microbiota, and host immunity. *Journal of Immunology (Baltimore, Md. : 1950)*, *195*(9), 4059–4066. https://doi.org/10.4049/jimmunol.1501432
Reynolds, L. A., Smith, K. A., Filbey, K. J., … Maizels, R. M. (2014). Commensal-pathogen interactions in the intestinal tract: Lactobacilli promote infection with, and are promoted by, helminth parasites. *Gut Microbes*, *5*(4), 522–532. https://doi.org/10.4161/gmic.32155
Roughgarden, J. (2020). Holobiont evolution: Mathematical model with vertical vs. horizontal microbiome transmission. *Philosophy, Theory, and Practice in Biology*, *12*(20220112), 20220112. https://doi.org/10.3998/ptpbio.16039257.0012.002
Roughgarden, J., Gilbert, S. F., Rosenberg, E., … Lloyd, E. A. (2017). Holobionts as units of selection and a model of their population dynamics and evolution. *Biological Theory*, *13*(1), 44–65. https://doi.org/10.1007/s13752-017-0287-1
Rubner, Y., Tomasi, C., & Guibas, L. J. (2000). The Earth Mover's Distance as a metric for image retrieval. *International Journal of Computer Vision*, *40*, 99–121. https://doi.org/10.1023/A:1026543900054
Salloum, P. M., Jorge, F., Dheilly, N. M., & Poulin, R. (2023a). Adoption of alternative life cycles in a parasitic trematode is linked to microbiome differences. *Biology Letters*, *19*(6), 20230091. https://doi.org/10.1098/rsbl.2023.0091
Salloum, P. M., Jorge, F., Dheilly, N. M., & Poulin, R. (2023b). Eco-evolutionary implications of helminth microbiomes. *Journal of Helminthology*, *97*, e22. https://doi.org/10.1017/S0022149X23000056
Sánchez, M. I., Georgiev, B. B., Nikolov, P. N., … Green, A. J. (2006). Red and transparent brine shrimps (*Artemia parthenogenetica*): A comparative study of their cestode infections. *Parasitology Research*, *100*(1), 111–114. https://doi.org/10.1007/s00436-006-0248-2
Sun, Y., Han, W., Liu, J., … Cheng, Y. (2020). Microbiota comparison in the intestine of juvenile Chinese mitten crab *Eriocheir sinensis* fed different diets. *Aquaculture*, *515*, 734518. https://doi.org/10.1016/j.aquaculture.2019.734518
Theis, K. R., Dheilly, N. M., Klassen, J. L., … Bordenstein, S. R. (2016). Getting the hologenome concept right: An eco-evolutionary framework for hosts and their microbiomes. *mSystems*, *1*(2), e00028–e00016. https://doi.org/10.1128/mSystems.00028-16
Thomas, F., Brodeur, J., Maure, F., … Rigaud, T. (2011). Intraspecific variability in host manipulation by parasites. *Infection, Genetics and Evolution*, *11*(2), 262–269. https://doi.org/10.1016/j.meegid.2010.12.013
Thomas, F., Schmidt-Rhaesa, A.A., Martin, G., … Renaud, F. (2002). Do hairworms (Nematomorpha) manipulate the water seeking behaviour of their terrestrial hosts? *Journal of Evolutionary Biology*, *15*(3), 356–361. https://doi.org/10.1046/j.1420-9101.2002.00410.x
Troscianko, J., & Stevens, M. (2015). Image calibration and analysis toolbox - a free software suite for objectively measuring reflectance, colour and pattern. *Methods in Ecology and Evolution*, *6*(11), 1320–1331. https://doi.org/10.1111/2041-210X.12439
Tsagou, V., Lianou, A., Lazarakis, D., … Aggelis, G. (2004). Newly isolated bacterial strains belonging to Bacillaceae (*Bacillus* sp.) and Micrococcaceae accelerate death of the honey bee mite, *Varroa destructor* (*V. jacobsoni*), in laboratory assays. *Biotechnology Letters*, *26*(6), 529–532. https://doi.org/10.1023/b:bile.0000019563.92959.0e
Tsuchida, T., Koga, R., Horikawa, M., … Fukatsu, T. (2010). Symbiotic bacterium modifies aphid body color. *Science*, *330*(6007), 1102–1104. https://doi.org/10.1126/science.1195463
Urbanek, S. (2022). png: Read and write PNG images. R. package. https://CRAN.R-project.org/package=png
Van Vliet, S., & Doebeli, M. (2019). The role of multilevel selection in host microbiome evolution. *Proceedings of the National Academy of Sciences*, *116*(41), 20591–20597. https://doi.org/10.1073/pnas.1909790116
Vance, S. A. (1996). Morphological and behavioural sex reversal in mermithid-infected mayflies. *Proceedings of the Royal Society of London. Series B: Biological Sciences*, *263*(1372), 907–912. https://doi.org/10.1098/rspb.1996.0134
Weller, H. I., & Westneat, M. W. (2019). Quantitative color profiling of digital images with earth mover's distance using the R package colordistance. *PeerJ*, *7*, e6398. https://doi.org/10.7717/peerj.6398
Wigglesworth, V. B. (1949). Insect biochemistry. *Annual Review of Biochemistry*, *18*(1), 595–614. https://doi.org/10.1146/annurev.bi.18.070149.003115
Yoon, J., Matsuo, Y., Matsuda, S., … Yokota, A. (2007). *Rubritalea spongiae* sp. nov. and *Rubritalea tangerina* sp. nov., two carotenoid- and squalene-producing marine bacteria of the family Verrucomicrobiaceae within the phylum 'Verrucomicrobia', isolated from marine animals. *International Journal of Systematic and Evolutionary Microbiology*, *57*(Pt 10), 2337–2343. https://doi.org/10.1099/ijs.0.65243-0
Zoetendal, E. G., Kapheim, K. M., Rao, V. D., … Robinson, G. E. (2015). Caste-specific differences in hindgut microbial communities of honey bees (*Apis mellifera*). *PLoS One*, *10*(4), e0123911. https://doi.org/10.1371/journal.pone.0123911
Zwirglmaier, K., Reid, W. D. K., Heywood, J., … Linse, K. (2014). Linking regional variation of epibiotic bacterial diversity and trophic ecology in a new species of Kiwaidae (Decapoda, Anomura) from East Scotia Ridge (Antarctica) hydrothermal vents. *Microbiology Open*, *4*(1), 136–150. https://doi.org/10.1002/mbo3.227